Synchrotron-radiation-based Mössbauer absorption spectroscopy with high resonant energy nuclides

Ryo Masuda [1] (ORCID) · Kohei Kusada [2] · Takefumi Yoshida [3] · Shinji Michimura [4] ·
Yasuhiro Kobayashi [1] · Shinji Kitao [1] · Hiroyuki Tajima [1] · Takaya Mitsui [5] ·
Hirokazu Kobayashi [2] · Hiroshi Kitagawa [2] · Makoto Seto [1,4,5]

Abstract

We successfully observed the synchrotron-radiation-based Mössbauer absorption spectra with ^{158}Gd and ^{99}Ru. Their nuclear resonant energies were 79.5 keV and 89.6 keV, respectively, and they are factually the highest energy which energy region synchrotron radiation covers with sufficient intensity as the incident X-rays for Mössbauer spectroscopy. Although the low recoilless fraction owing to these high resonant energy, Mössbauer energy spectra of GdPd$_3$ to ^{158}Gd$_2$O$_3$ and fcc-Ru nanoparticles to bulk hcp-^{99}Ru metal were obtained with natural samples of the former compounds with sufficient amount, because of the high transparency of these high energy X-rays(to electronic scattering). In spite of large statistical errors, we can evaluate the hyperfine parameters when the spectrum includes simple 1-site profile. ^{99}Ru and ^{158}Gd SR-based Mössbauer absorption spectra of various complex materials including somewhat complex structures will be available with the improvements to the measurement system; More detector elements for larger solid angle subtended to the scatterer sample will yields more counting rates and improvement higher recoilless fraction by arranging more appropriate chemical specimen as the scatterer yields deeper absorption profile.

Keywords Synchrotron-radiation-based Mössbauer absorption spectroscopy · ^{99}Ru · ^{158}Gd · Nuclear resonant scattering

✉ Ryo Masuda
  masudar@rri.kyoto-u.ac.jp; masudar@hirosaki-u.ac.jp

Extended author information available on the last page of the article

1 Introduction

Mössbauer spectroscopy have been used as a powerful and unique method in various fields, such as physics, chemistry, biology, and earth science [1]. Mössbauer effect, the principle of this method, was first discovered using the nuclear resonance of ^{191}Ir, and the effect has been observed for 86 nuclides of 45 elements [2]. Among them, ^{57}Fe and ^{119}Sn are the most well-known Mössbauer nuclides and most Mössbauer spectra have been observed with these two nuclides. For these two nuclides, we can purchase the γ-ray sources, that is, corresponding radioactive isotopes (RI). However, RI sources for the other nuclides cannot usually be purchased and thus the preparation of RI sources is one large difficulty in Mössbauer spectroscopy of those nuclides. In spite of this difficulty, many researchers made those sources using a nuclear reactor and/or particle accelerator to observe the Mössbauer spectra of various nuclides [1]. In 1970's, the synchrotron radiation (SR) was considered as a potential source for Mössbauer spectroscopy [3, 4] and successfully used to the measurement of hyperfine structure in 1985 [5]. The white energy property of SR, extending to typically 100 keV, was consider to be suitable to Mössbauer spectroscopy of those nuclides, as well as its high brilliance, low angular divergence, and high polarization are also suitable to the Mössbauer study for various samples under various situations, such as high pressure and in-situ gas atmosphere. Using SR, Mössbauer experiments with nuclides whose resonant energy is below 100 keV is available and until now, nuclear resonant forward scattering (NFS) experiments [6] have been actively performed with these nuclides. Even so, the Mössbauer experiments using high-energy nuclear resonance is difficult owing to the low recoilless fraction caused by the high recoil energy and at least one magnitude lower intensity than that around 10 keV even at the third generation facility. Furthermore, the high resolution monochromator to extract the X-rays with the bandwidth of some meV is practically effective only for X-rays below 40 keV [7–9]. Despite, the time spectra of NFS by ^{61}Ni [10–12] (the nuclear resonant energy E_{res} = 67.4 keV), ^{99}Ru [13] (E_{res} = 89.6 keV), and ^{193}Ir [14] (E_{res} = 73.0 keV) were successfully observed. Another possible SR-using Mössbauer method for these high resonant energy nuclides is SR-based Mössbuer absorption spectroscopy [15]. As for this method, Mössbauer energy spectra of ^{61}Ni [16–19] and ^{174}Yb (E_{res} = 76.5 keV) were successfully observed [20, 21]. Here, we report the feasibility study of the SR-based Mössbauer absorption spectroscopy with other two nuclides whose nuclear resonant energy was higher than those of nuclides performed by this method before: ^{158}Gd (E_{res} = 79.5 keV) and ^{99}Ru. In addition, the recent ^{61}Ni measurement by this method is also shortly discussed for comparison; ^{61}Ni is a relatively major nuclide in Mössbauer spectroscopy using SR among nuclides with high nuclear resonance and a good reference to the SR Mössbauer study using new high-energy nuclides.

2 Typical SR-based Mössbauer absorption spectroscopy: ^{61}Ni case

Here, the functionality of the instrumentation in SR-based Mössbauer absorption spectroscopy is discussed using an example of most recent ^{61}Ni case. This typical experiments were performed in BL11XU of SPring-8. The schematic drawing of the general experimental instrumentation of this method is shown in Fig. 1. The electron bunch-mode of the storage ring was 203 bunch mode, where the period of each electron bunches were 23.6 ns. The SR from the undulator was monochromatized by the Si (3 3 3) high heat load monochromator (HHLM). The SR transmitted another Si (1 1 1) channel-cut crystal to eliminate the low energy

SR corresponding to the lower-index reflection of HHLM. The intensity of the SR was 3.6 μA by a positive-intrinsic-negative (PIN) photodiode detector with 0.7 mm thickness. Then the SR penetrated the transmitter sample, 1 mm of the polycrystalline natural (i. e., non-enriched) Ni metal in this case. It was arranged into a helium cryostat and its temperature was 20 K. Then, SR was then incident on the scatterer, an enriched $^{61}Ni_{0.86}V_{0.14}$ foil. The enrichment of the foil was 86.2% and its thickness was 3.1 μm. It was 30 degree inclined to the beam direction. The effective thickness of the scatterer was 4 using the Debye model with recoilless fraction in ref. 22 and the energy width due to the effective thickness was around $2\Gamma_0$, where Γ_0 is natural linewidth of ^{61}Ni and 0.38 mm/s. Here we also note that the main detected scattering was internal conversion (IC) electrons. Electrons maximum penetration length is by far smaller than the attenuation length of X-rays with the same energy, and it often limits the actual thickness. In ^{61}Ni case, this length was 8 μm, which was larger than the real thickness of this foil and not limits the actual thickness. In addition, it shows no hyperfine splitting. It was arranged into a vacuum chamber and cooled down to around 60 K by a refrigerator. It was also connected with a Mössbauer velocity transducer to control the energy of its nuclear resonance through a Doppler effect of light. The velocity was calibrated by a Mössbauer laser velocity calibrator. The scattering from the scatterer was detected by an array of eight avalanche photo diode (APD) detector elements [23, 24], which was arranged in the same vacuum chamber to detect the nuclear resonantly scattered electrons through the IC process from the scatterer [20, 25]. The Mössbauer energy spectrum was measured as follows: the SR penetrating the transmitter showed an absorption profile corresponding to the hyperfine structure of the transmitter. Therefore, the nuclear resonant scattering intensity from the scatterer was absent when the nuclear resonance energy of the scatterer, which is controlled by the transducer, was coincide with the energy of the transmitter, while it was intense when the resonant energies of the transmitter and the scatterer were different. This is the basic functionality of the measurement system for the SR-based Mössbauer absorption spectroscopy. We note that one of the transmitter and the scatterer is a sample under study and the other is energy analyzer. The analyzer should usually show a simple single-line profile without (at least apparent) hyperfine splitting. We also note that the effective thickness of the scatterer should not be by far thicker than that of the transmitter, because the absorption in the spectra become shallow. In this viewpoint, the relation between the transmitter and the scatterer resembles to that between the sample and the γ-ray source at conventional RI Mössbauer spectroscopy.
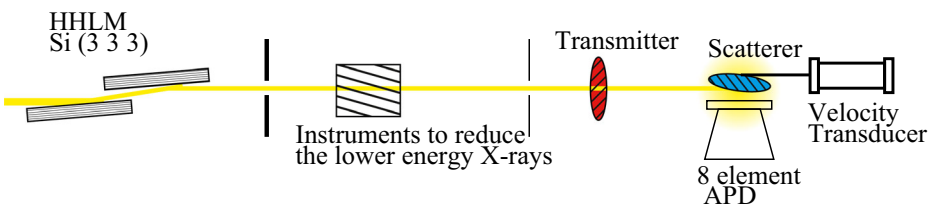

Fig. 1 Schematic drawing of the measurement system for SR-based Mössbauer absorption spectroscopy. In the case of ^{61}Ni, the instruments to reduce the lower energy X-rays were a Si (1 1 1) channel-cut monochromator, the transmitter was bulk Ni metal, and the scatterer was a Ni-V alloy. In the case of ^{158}Gd, the instruments to reduce the lower energy X-rays were Cu and Pb attenuator, the transmitter was $GdPd_3$, and the scatterer was Gd_2O_3. In the case of ^{99}Ru, the instruments to reduce the lower energy X-rays were Cu attenuator and Si(1 1 1) monochromator, the transmitter was fcc-Ru NPs, and the scatterer was bulk hcp-Ru
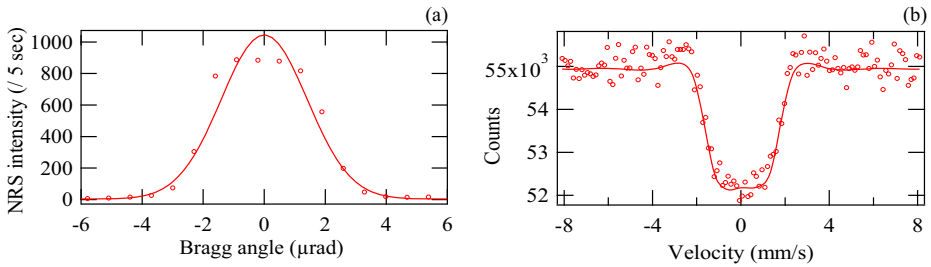
Fig. 2 The results of SR-based Mössbauer absorption spectroscopy using ^{61}Ni. **a** The intensity dependence on the Bragg angle of HHLM. **b** The Mössbauer spectrum of Ni metal vs Ni-V alloy. The open circles are experimental data and the lines are fitting curve in both figures

The intensity of the ^{61}Ni nuclear resonance detected by the APD detector was 200 counts per seconds (cps) with the noise level of 0.7 cps, as shown Fig. 2a. This is about 1.5 times higher counting rate than that in ref. 16; this is because of some fine tunings of the measurement system. The main of the improvements is the distance between the scatter foil and the detector decreased from 4 mm in ref. 16 to 3.5 mm in this experiment by the improvement of the shape of the detector package, resulting in the larger solid angle for the detector subtended at the scatter. With this counting rate, the SR-based Mössbauer absorption spectra of Ni metal vs Ni-V alloy was measured, as shown in Fig. 2b. An analyzable spectrum is obtained in 12 h measurement, which is 2/3 of the ref. 16.

3 ^{158}Gd SR-based Mössbauer absorption spectroscopy

The conventional Mössbauer spectroscopy with Gd element has been usually performed using ^{155}Gd second excited state [26]. This nuclides has moderate natural abundance of 14.8%, and this excited state has moderate nuclear resonant energy of 86.5 keV and moderate energy width corresponding to the half-life of 6.5 ns. Especially, the RI source of ^{155}Sm is *relatively* easy to prepare by neutron irradiation to ^{154}Sm, the heaviest stable isotope of Sm element with its natural abundance of 22.7%. This source is also *relatively* easy to treat due to the long half-life of 4.7 years of ^{155}Eu in the decay process. Thus, conventional Mössbauer spectroscopy using this RI source has been performed with ^{155}Gd nuclides. In the viewpoint of the natural abundance and nuclear resonant energy, ^{158}Gd first excited state is better: those were 24.8%
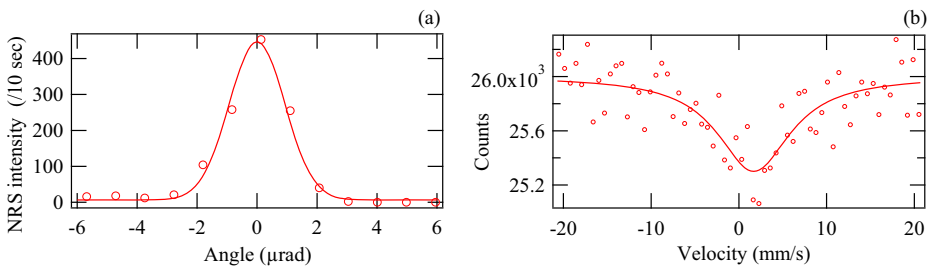

Fig. 3 The results of SR-based Mössbauer absorption spectroscopy using ^{158}Gd. **a** The intensity dependence on the Bragg angle of HHLM. **b** The Mössbauer spectrum of GdPd$_3$ vs Gd$_2$O$_3$. The open circles are experimental data and the lines are fitting curve in both figures

and 79.5128 (15) keV, respectively [27]. The highest natural abundance of around 1/4 among Gd nuclides is advantageous in the Mössbauer experiments using natural samples and lower resonant energy causes relatively higher recoilless fraction. For example, the recoilless fraction is 0.19 at 20 K for ^{158}Gd while it is 0.14, in the case of the Debye temperature of 237 K, corresponding to GdPd$_3$ alloy [28]. Its half-life of 2.52 (3) ns [27] is a drawback. However, the preparation of RI source is quite difficult; there is no *relatively* convenient way to synthesize the sufficiently intense RI source for this nuclide. Consequently, the source was prepared by in-beam method, in which the enriched ^{157}Gd parent compounds was continuously irradiated by neutron beam during the experimental period [29, 30]. We can overcome this difficulty using SR and thus ^{158}Gd is another choice for SR experiments. In fact, nuclear resonant scattering (NRS) of SR by ^{158}Gd was already measured with low intensity [31]. (Note that the measured NRS is incoherent NRS and not NFS.) Therefore, we developed a ^{158}Gd SR-based Mössbauer absorption measurement system.

The experiments were also performed in BL11XU of SPring-8. The arrangement of the experiment was similar one shown in Fig. 1. The electron bunch-mode of the storage ring was the 203 bunch mode and the SR from the undulator was monochromatized by the Si (3 3 3) HHLM. Then, the SR transmitted the Pb and Cu attenuator to reduce the low energy SR corresponding to the Si (1 1 1) reflection of HHLM. We did not use an additional Si crystal monochromator according to the high energy NFS experiment of ^{99}Ru [13]. The intensity of the SR was 0.5 μA by the PIN photodiode detector here. Then the SR penetrated the transmitter sample, GdPd$_3$. The GdPd$_3$ is similar compounds to SmPd$_3$, which had been used as a RI source in conventional ^{155}Gd Mössbauer spectroscopy; it shows only simple single-line absorption profile in the conventional method. The GdPd$_3$ sample was natural and 79.5 mg of that sample was shaped into the pellet with the diameter of 5 mm. It was arranged into a helium cryostat and its temperature was 10 K, just above the Néel temperature of 7.5 K [32]. SR was then incident on the scatterer, another pellet of Gd$_2$O$_3$. 14 mg of the 97.7% enriched powder was shaped into 7 mm diameter and the pellet was 8 degree inclined to the beam direction. It was arranged into a vacuum chamber, cooled down to around 70 K by a refrigerator, and connected with the Mössbauer velocity transducer, whose velocity was calibrated by the Mössbauer laser velocity calibrator. The effective thickness of the scatterer was 6×10^1 using the Debye temperature in ref. 33. However, because the main detected scattering component was IC electrons, this real thickness was too large considering the maximum electron penetration length, which corresponds to the effective thickness of 5. The energy width due to this effective thickness was around $2\Gamma_0$, where Γ_0 of ^{158}Gd is 0.68 mm/s, assuming this scatterer shows no hyperfine splitting with single crystallographic site. In fact, both assumption was wrong, as described later. The scattering from the scatterer was detected by the 8-element array APD.

The intensity of the nuclear resonance at the APD detector was 44 cps with the noise level of 0.6 cps, as shown Fig. 3a. This was one-hundred times higher intensity than that reported in the previous NRS experiment [31]. Comparing with this literature, we had mainly three improvements: first, the Gd$_2$O$_3$ was enriched sample in this experiment and thus the density of the resonant nuclei was four times of that in the previous NRS experiment. Second, the IC electrons are detected in this experiment and the IC coefficient of the decay process of ^{158}Gd first excited state is 6.02 [27]. In contrast, only the fluorescent X-rays following the IC process were detected in the previous experiment. The detection efficiency of APD was much higher to

IC electrons. Third, the solid angle for the APD detector subtended at the scatterer was larger because eight element APD array was arranged in this experiment although one smaller element APD was arranged in the previous experiment.

The SR-based Mössbauer absorption spectra of $GdPd_3$ vs Gd_2O_3 is shown in Fig. 3b. We can see the absorption profile. The line in Fig. 3b is written based on an evaluation by one single Lorentzian, which is too simple to analyze the spectrum of Gd_2O_3; this oxide forms the bixbyite structure, where Gd atom occupies two different crystallographic sites, 8a and 24d. Thus, we should analyze the spectrum using two components with nuclear quadrupole splitting, which were shown by [155]Gd RI Mössbauer spectroscopy [34]. Thus, this spectrum includes two pairs of three absorption lines, reflecting to the 2+ (first) → 0 (ground) nuclear transition. Unfortunately, the statistical errors in the spectrum is not enough for this kind of analysis, in spite of the improved intensity and long measurement time of 30 h. The broad FWHM of 10 ± 2 mm/s still supports the existence of some hyperfine structure. This is because in the case the spectrum shows no hyperfine structure, the FWHM should be at most 3.4 mm/s considering the effective thickness evaluated using the recoilless fraction based on the Debye temperatures reported in ref. 34 for $GdPd_3$ and ref. 33 for Gd_2O_3.

4 [99]Ru SR-based Mössbauer absorption spectroscopy

The [99]Ru conventional Mössbauer spectroscopy has been usually performed since the first experiment by Kistner [35], although the nuclides has some undesirable properties: the natural abundance of [99]Ru is only 12.7% and the recoilless fraction of samples were often low owing to the high energy of the first excited state of [99]Ru, 89.57 (6) keV [36]. One superior property is its narrow energy width corresponding to the half-life of the excited, 20.5 (1) ns [36]. The width is narrow enough to evaluate the valence via the isomer shift. The RI source in the conventional method was [99]Rh, which was synthesized by *relatively* convenient [99]Ru (*p*, *n*) [99]Rh reaction and the 16 days half-life of [99]Rh is also *relatively* convenient to handle it. As for SR method, NFS of this nuclides was already observed [13] and this is the highest energy nuclear resonance that is observed using SR methods. We also tried the SR-based Mössbauer absorption spectroscopy using this highest energy nuclear resonance.

The experiments were also performed in BL11XU of SPring-8 and the arrangement of the experiment was also similar one shown in Fig. 1. The electron bunch-mode of the storage ring was also the 203 bunch mode. The SR from the undulator was monochromatized by the Si (3 3 3) HHLM. Then, the SR penetrated the Cu attenuator and was diffracted by another Si(1 1 1) monochromator to eliminate the low energy SR. The intensity of the SR was 0.3 μA by the PIN photodiode detector here. Then the SR penetrated the transmitter sample, natural Ru nanoparticles (NP). These Ru NPs formed a face-centered cubic (fcc) structure, which is different from the bulk Ru structure, hexagonal closed packed (hcp) structure. The average size of the NPs were 2.6 ± 0.5 nm. These NPs were synthesized by the chemical reduction method, described in the literature [37, 38]. This sample was natural and the NPs including 100.4 mg Ru component was shaped into the pellet with the diameter of 5 mm. It was arranged into a helium cryostat and its temperature was 4 K. SR is then incident on the scatterer, bulk hcp-Ru metal. 19.7 mg of the 95.5% enriched [99]Ru bulk powder was shaped into 7 mm diameter and the pellet was 8 degree inclined to the beam direction. It is arranged into a vacuum chamber and cooled down to around 45 K by a refrigerator. It is also connected with the Mössbauer

velocity transducer, whose velocity was calibrated by the Mössbauer laser velocity calibrator. The effective thickness of the scatterer was 3×10^1 using the Debye temperature in ref. 13. However, because the main detected scattering component was IC electrons and this thickness was too large considering the maximum electron penetration length, which corresponds to the effective thickness of 7 and the energy width due to this effective thickness was around $3\Gamma_0$, where Γ_0 of ^{99}Ru is 7.4×10^{-2} mm/s. This scatterer showed no hyperfine splitting. The scattering from the scatterer was detected by an array of eight APD detectors.

The intensity of the nuclear resonance detected by the APD detector was 3 cps with the noise level of 0.1 cps, as shown Fig. 4a. With this counting rate, the SR-based Mössbauer absorption spectra of fcc-Ru NPs vs bulk hcp-Ru was measured, as shown in Fig. 4b. Although it takes 72 h to measure the spectrum, the statistical errors in the spectrum is also not small, similar to the ^{158}Gd spectrum. Even in such case, we can evaluate the hyperfine structure with the following reasonable assumption: fcc-Ni NPs showed neither quadrupole splitting nor magnetic hyperfine structure, because bulk hcp-Ru showed none of these hyperfine structures [13, 39]. The isomer shift was estimated to be -0.04 ± 0.06 mm/s under this assumption and the valence state of fcc-Ru NP is not different from that of bulk hcp-Ru in the experimental error. Considering the typical isomer shift values shown in ref. 40, where the typical isomer shift differences corresponding one electric valence (for example, between Ru^{3+} and Ru^{4+}) was more than 0.1 mm/s, we can discuss the valence states of Ru atom through this spectrum. The FWHM of 0.5 ± 0.3 mm/s is also reasonable when we consider the effective thickness of the samples using the recoilless fraction of Ru metal based on ref. 13. Recently, Ru thin films with its thickness of 2.5–12 nm forming body-centered tetragonal (bct) structure shows the ferromagnetism even at room temperature [41], but we cannot detect such magnetization in this fcc-Ru NPs in spite of their smaller size.

5 Discussion

Because we successfully observed SR-based Mössbauer absorption spectra with ^{158}Gd and ^{99}Ru using natural transmitters, the third generation SR is available for SR-based Mössbauer absorption spectroscopy with nuclides whose resonant energy is below 90 keV. However, these spectra were not clear enough to analyze the fine structure in the spectra, although it takes more than 1 day to measure one spectrum. This situation should be improved to measure
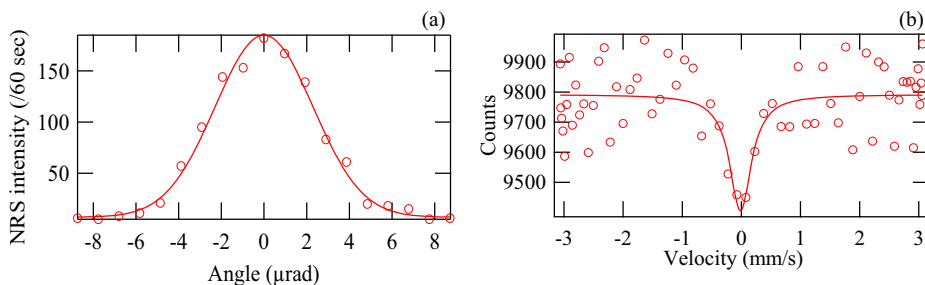

Fig. 4 The results of SR-based Mössbauer absorption spectroscopy using ^{99}Ru. **a** The intensity dependence on the Bragg angle of HHLM. **b** The Mössbauer spectrum of fcc-Ru NP vs bulk hcp-Ru. The open circles are experimental data and the lines are fitting curve in both figures

the Mössbauer energy spectra of various actual samples in all kinds of scientific field and could be improved, if we optimize the measurement system as the ^{61}Ni situation. Considering the actual applicability, the expensive enriched transmitter samples are not a desirable way. One way for the improvement is reconsider the chemical compounds of the scatterer as the energy reference sample. In these experiments, the recoilless fraction of the scatterers, Gd_2O_3 and hcp-Ru metal, was estimated to be 0.28 and 0.18, respectively. Thus, there remains large space to enhance the fraction and this problem is common to all high-energy nuclides. The recoilless fraction strongly relates to the characteristic temperature of the chemical compounds reflecting the atomic bonding strength around the Mössbauer atoms, like the Debye temperature and thus the good scatterer with such high characteristic temperature enhance the Mössbauer effect. One candidate is dodeca-boride compounds, which showed good recoilless fraction in Yb SR-based Mössbauer absorption spectroscopy, about 0.4 for 76.4 keV ^{174}Yb nuclear resonance. However, GdB_{12} was synthesized only under high pressure [42] and thus future effort should be required. Another way for the improvement is on the detector. In fact, the size of each element in the APD array was 3×5 mm in the area with the depletion layer of 150 μm. An APD array with more elements can cover a larger solid angle. Furthermore, there also remains a subject to consider on the elimination of low energy X-rays. As is also discussed in ref. 13, the transmitter sample itself might be the attenuator to lower energy X-rays in some cases. If the attenuators were removed in these our SR-based Mössbauer measurements, at least three times intensity could be available. However, in that case, the scattering intensity might be too strong to our APD detectors. Thus, increasing the APD elements will be also a solution to this problem.

Lastly, we discuss the comparison with the NFS method. In fact, for ^{61}Ni and ^{99}Ru, the NFS measurements have been also performed. NFS spectra are usually measured in shorter time and the hyperfine parameters can be usually obtained more precisely by NFS. In contrast, the SR-based Mössbauer absorption spectra are intuitively understand because they are energy spectra of hyperfine structures, familiar to Mössbauer scientist using conventional RI method. This is important when the sample is unknown or not simple; at least, the difference of some parameters (e.g. temperature) or from the standard sample can be discussed using the change of the center of gravity of the spectra, the width of broadened absorption, and so forth. This situation is seen in ^{61}Ni experiments; the NFS produced the excellent results on the change of known single-site samples under high pressures and SR-based Mössbauer spectroscopy was applied to somewhat complex samples like Li battery materials. The best way is to measure both spectra. SR-based Mössbauer absorption spectra yields an appropriate analyzing model and reasonable fitting initial values for NFS spectra, which shows precise hyperfine parameters with an unambiguous fitting model.

6 Summary

The SR-based Mössbauer absorption spectra with ^{158}Gd and ^{99}Ru were successfully observed in spite of their high nuclear resonant energy. This shows that we can obtain the SR-based Mössbauer absorption spectra with nuclides whose nuclear resonant energy is around 90 keV, even if the transmitter samples are composed of non-enriched elements. However, the statistical errors were not sufficiently low when we analyze some complex structure, as is in the case of Gd_2O_3, which has two crystallographic sites showing nuclear quadrupole splitting. In contrast, when the sample shows only one-site absorption, we can discuss the hyperfine

parameters; the fcc-Ru NPs showed the same isomer shifts as that of bulk hcp-Ni within the reasonable experimental error. The enhancement of the recoilless fraction of the scatterer sample and counting rates are important to apply this method to various samples including [158]Gd and [99]Ru, which often includes many sites. Increasing the number of APD element is promising method to obtain sufficient experimental counts.

References

1. Gütlich, P., Bill, E., Trautwein, A.X.: Mössbauer Spectroscopy and Transition Metal Chemistry. Springer, Berlin (2011)
2. Website of the Mössbauer Effect Data Center. http://www.medc.dicp.ac.cn/Resources.php (2019). Accessed 21 August 2019
3. Ruby, S.L.: Mössbauer experiments without conventional sources. J. Phys. (Paris), Colloq. **35**, C6–209–C6–211 (1974)
4. Cohen, R.L., Miller, G.L., West, K.W.: Nuclear resonance excitation by synchrotron radiation. Phys. Rev. Lett. **41**, 381–384 (1978)
5. Gerdau, E., Rüffer, R., Winkler, H., Tolksdorf, W., Klages, C.P., Hannon, J.P.: Nuclear Bragg diffraction of synchrotron radiation in yttrium iron garnet. Phys. Rev. Lett. **54**, 835–838 (1985)
6. Hastings, J.B., Siddons, D.P., van Bürck, U., Hollatz, R., Bergmann, U.: Mössbauer spectroscopy using synchrotron radiation. Phys. Rev. Lett. **66**, 770–773 (1991)
7. Wille, H.-C., Shvyd'ko, Y.V., Alp, E.E., Rüter, H.D., Leupold, O., Sergueev, I., Rüffer, R., Barla, A., Sanchez, J.P.: Nuclear resonant forward scattering of synchrotron radiation from [121]Sb at 37.13 keV. Europhys.Lett. **74**, 170–176 (2006)
8. Imai, Y., Yoda, Y., Kitao, S., Masuda, R., Higashitaniguchi, S., Inaba, C., Seto, M.: High-energy-resolution monochromator for nuclear resonant scattering of synchrotron radiation by Te-125 at 35.49 keV. Proc. SPIE. **6705**, 670512 (2007)
9. Sergueev, I., Wille, H.-C., Hermann, R.P., Bessas, D., Shvyd'ko, Y.V., Zając, M., Rüffer, R.: Milli-electronvolt monochromatization of hard X-rays with a sapphire backscattering monochoromator. J. Synchrotron Radiat. **18**, 802–810 (2011)
10. Sergueev, I., Chumakov, A.I., Deschaux, T.H., Rüffer, R., Strohm, C., van Bürck, U.: Nuclear forward scattering for high energy Mössbauer transitions. Phys. Rev. Lett. **99**, 097601 (2007)
11. Sergueev, I., Dubrovinsky, L., Ekholm, M., Vekilova, O.Y., Chumakov, A.I., Zajac, M., Potapkin, V., Kantor, I., Bornemann, S., Ebert, H., Simak, S.I., Abrikosov, I.A., Rüffer, R.: Hyperfine splitting and room temperature ferromagnetism of Ni at multimegabar pressure. Phys. Rev. Lett. **111**, 157601 (2013)
12. Sobelev, A.V., Glazkova, I.S., Akulenko, A.A., Sergueev, I., Chumakov, A.I., Yi, W., Belik, A.A., Presniakov, I.A.: [61]Ni nuclear forward scattering study of magnetic hyperfine interactions in double perovskite A_2NiMnO_6 (A=Sc, In, Tl). J. Phys. Chem. C. 23628–23634 (2019)
13. Bessas, D., Merkel, D.G., Chumakov, A.I., Rüffer, R., Hermann, R.P., Sergueev, I., Mahmoud, A., Klobes, B., McGuire, M.A., Sougrati, M.T., Stievano, L.: Nuclear forward scattering of synchrotron radiation by [99]Ru. Phys. Rev. Lett. **113**, 147601 (2014)
14. Alexeev, P., Leupold, O., Sergueev, I., Herlitschke, M., McMorrow, D.F., Perry, R.S., Hunter, E.C., Röhlsberger, R., Wille, H.-C.: Nuclear resonant scattering from [193]Ir as a probe of the electronic and magnetic properties of iridates. Sci. Rep. **9**, 5097 (2019)
15. Seto, M., Masuda, R., Higashitaniguchi, S., Kitao, S., Kobayashi, Y., Inaba, C., Mitsui, T., Yoda, Y.: Synchrotron-radiation-based Mössbauer spectroscopy. Phys. Rev. Lett. **102**, 217602 (2009)

16. Masuda, R., Kobayashi, Y., Kitao, S., Kurokuzu, M., Saito, M., Yoda, Y., Mitsui, T., Hosoi, K., Kobayashi, H., Kitagawa, H., Seto, M.: ^{61}Ni synchrotron radiation-based Mössbauer spectroscopy of nickel-based nanoparticles with hexagonal structure. Sci. Rep. **6**, 20861 (2016)

17. Segi, T., Masuda, R., Kobayashi, Y., Tsubota, T., Yoda, Y., Seto, M.: Synchrotron radiation-based ^{61}Ni Mössbauer spectroscopic study of Li(Ni$_{1/3}$Mn$_{1/3}$Co$_{1/3}$)O$_2$ cathode materials of lithium ion rechargeable battery. Hyperfine Interact. **237**(7), (2016)

18. Gee, L.B., Lin, C.-Y., Jenney Jr., F.E., Adams, M.W.W., Yoda, Y., Masuda, R., Saito, M., Kobayashi, Y., Tamasaku, K., Lerche, M., Seto, M., Riordan, C.G., Ploskonka, A., Power, P.P., Cramer, S.P., Lauterbach, L.: Synchrotron-based nickel Mössbauer spectroscopy. Inorg. Chem. **55**, 6866–6872 (2016)

19. Masuda, R., Kobayashi, H., Aoyama, Y., Saito, M., Kitao, S., Ishibashi, H., Hosokawa, S., Mitsui, T., Yoda, Y., Kitagawa, H., Seto, M.: ^{61}Ni synchrotron-radiation-based Mössbauer absorption spectroscopy of Ni nanoparticle composites. Hyperfine Interact. **239**(11), (2018)

20. Masuda, R., Kobayashi, Y., Kitao, S., Kurokuzu, M., Saito, M., Yoda, Y., Mitsui, T., Iga, F., Seto, M.: Synchrotron radiation-based Mössbauer spectra of ^{174}Yb measured with internal conversion electrons. Appl. Phys. Lett. **104**, 082411 (2014)

21. Oura, M., Ikeda, S., Masuda, R., Kobayashi, Y., Seto, M., Yoda, Y., Hirao, N., Kawaguchi, S., Ohishi, Y., Suzuki, S., Kuga, K., Nakatsuji, S., Kobayashi, H.: Valence fluctuating compound α-YbAlB4 studied by ^{174}Yb Mössbauer spectroscopy and X-ray diffraction using synchrotron radiation. Physica B. **536**, 162–164 (2018)

22. Love, J.C., Obenshain, F.E., Czjzek, G.: Mössbauer spectroscopy with ^{61}Ni in nickel-transition-metal alloys and nickel compounds. Phys. Rev. B. **3**, 2827–2840 (1971)

23. Kishimoto, S.: An avalanche photodiode detector for X-ray timing measurements. Nucl. Instrum. Meth. Phys. Res. A. **309**, 603–605

24. Kishimoto, S., Yoda, Y., Seto, M., Kitao, S., Kobayashi, Y., Haruki, R., Harami, T.: Array of avalanche photodiodes as a position-sensitive X-ray detector. Nucl. Instrum. Meth. Phys. Res. A. **513**, 193–196 (2003)

25. Kishimoto, S., Yoda, Y., Seto, M., Kobayashi, Y., Kitao, S., Haruki, R., Kawauchi, T., Fukutani, K., Okano, T.: Observation of nuclear excitation by electron transition in ^{197}Au with synchrotron X rays and an avalanche photodiode. Phys. Rev. Lett. **85**, 1832–1834 (2000)

26. Czjzek, G.: Mössbauer spectroscopy of new materials containing gadolinium. Mössbauer spectroscopy applied to magnetism and materials science, vol. 1, Chap. 9, 373–429. Plenum press, New York (1993)

27. Helmer, R.G.: Nuclear data sheets for A=158. Nuclear Data Sheets. **101**, 325–519 (2004)

28. Pandey, A., Mazumdar, C., Ranganathan, R., Johnston, D.C.: Multiple crossovers between positive and negative magnetoresistance versus field due to fragile spin structure in metallic GdPd$_3$. Sci. Rep. **7**, 42789 (2017)

29. Fink, J., Kienle, P.: Recoilless γ emission in ^{156}Gd and ^{158}Gd following neutron capture reaction. Phys. Lett. **17**, 326–327 (1965)

30. Fink, J.: Mössbauereffektmessungen am 79,5 keV-Niveau von Gd^{158}. Z. Phys. **207**, 225–234 (1967)

31. Mitsui, T., Masuda, R., Kitao, S., Seto, M.: Nuclear resonant scattering of synchrotron radiation by ^{158}Gd. J. Phys. Soc. Jpn. **74**, 3122–3123 (2005)

32. Gardner, W.E., Penfold, J., Smith, T.F., Harris, I.R.: The magnetic properties of rare earth-Pd$_3$ phases. J. Phys. F Metal Phys. **2**, 133–150 (1972)

33. We assumed that the Debye temperature of cubic Gd$_2$O$_3$ is similar to that of monoclinic one. Haglund, J. A., Hunter, J. R.: Elastic properties of polycrystalline monoclinic Gd$_2$O$_3$. J. Am. Ceram. Soc. 56, 327–330 (1973)

34. Bauminger, E.R., Froindlich, D., Mustachi, A., Nowik, I., Ofer, S., Samuelov, S.: Magnetic and quadrupole moments of the 86.5 keV excited state of ^{155}Gd. Phys. Lett. B. **30**, 531–532 (1969)

35. Kistner, O.C., Monaro, S., Segnan, R.: Recoilless resonance absorption in Ru^{99}. Phys. Lett. **5**, 299 (1963)

36. Brownie, E., Tuli, J.K.: Nuclear data sheets for a=99. Nuclear Data Sheets. **145**, 25–340 (2017)

37. Kusada, K., Kobayashi, H., Yamamoto, T., Matsumura, S., Sumi, N., Sato, K., Nagaoka, K., Kubota, Y., Kitagawa, H.: Discovery of face-centered cubic ruthenium nanoparticles: facile size-controlled synthesis using the chemical reduction method. J. Am. Chem. Soc. **135**, 5493–5496 (2013)

38. Kumara, L.S.R., Sakata, O., Kohara, S., Yang, A., Song, C., Kusada, K., Kobayashi, H., Kitagawa, H.: Origin of the catalytic activity of face-centered cubic ruthenium nanoparticles determined from an atomic-scale structure. Phys. Chem. Chem. Phys. **18**, 30622 (2016)

39. Kistner, O.C.: Recoil-free absorption hyperfine spectra of the 90-keV mixed transition in Ru^{99}. Phys. Rev. **144**, 1022–1030 (1966)

40. Kaindl, G., Potzel, W., Wagner, F., Zahn, U., Mössbauer, R.L.: Isomer shifts of the 90 keV γ-rays of ^{99}Ru in ruthenium compounds. Z. Phys. **226**, 103–115 (1969)

41. Quarterman, P., Sun, C., Garcia-Barriocanal, J., Mahendra, D.C., Yang, L., Manipatruni, S., Nikonov, D.E., Young, I.A., Voyles, P.M., Wang, J.-P.: Demonstration of Ru as the 4th ferromagnetic element at room temperature. Nat. Comm. **9**, 2058 (2018)
42. Cannon, J.F., Cannnn, D.M., Hall, H.T.: High pressure synthesis of SmB_2 and GdB_{12}. J. Less Comm. Met. **56**, 83–90 (1977)

Publisher's note   Springer Nature remains neutral with regard to jurisdictional claims in published maps and institutional affiliations.

Affiliations

Ryo Masuda[1] · **Kohei Kusada**[2] · **Takefumi Yoshida**[3] · **Shinji Michimura**[4] · **Yasuhiro Kobayashi**[1] · **Shinji Kitao**[1] · **Hiroyuki Tajima**[1] · **Takaya Mitsui**[5] · **Hirokazu Kobayashi**[2] · **Hiroshi Kitagawa**[2] · **Makoto Seto**[1,4,5]

[1]   Institute for Integrated Radiation and Nuclear Science, Kyoto University, 2-1010, Asashironishi, Kumatori-cho, Sennan-gun, Osaka 590-0494, Japan

[2]   Division of Chemistry, Graduate School of Science, Kyoto University, Kitashirakawa Oiwakecho, Sakyo-ku, Kyoto 606-8502, Japan

[3]   Electronic Functional Macromolecules Group, National Institute for Materials Science, 1-1 Namiki, Tsukuba, Ibraki 304-0044, Japan

[4]   Graduate School of Science and Engineering, Saitama University, 225 Simo-Okubo, Sakura-ku, Saitama 338-8570, Japan

[5]   Synchrotron Radiation Research Center, Kansai Photon Science Institute, Quantum Beam Science Research Directorate, National Institutes for Quantum and Radiological Science and Technology, 1-1-1, Kouto, Sayo-cho, Sayo-gun, Hyogo 679-5148, Japan